

Chapter 8

Map of Achievable Performance (MAP)



The *MAP approach* provides a way to analyze the steady-state handling behavior of road/race cars. It is completely general, in the sense that it can be employed for any real car, and for any mathematical model as well.

Two concepts play a central role in MAP: the *achievable region*, that is the totality of the achievable trim conditions for a given vehicle, and the *level (handling) curves* inside the achievable region, to highlight the vehicle peculiar features.

The envelope of level curves is often a good practical way to obtain the achievable regions, as will be shown shortly.

8.1 MAP Fundamental Idea

The MAP approach for road cars has been introduced in Sect. 6.8, and employed in Sect. 6.10 (see also p. 231). For race cars, the MAP approach has been briefly discussed in Sect. 7.6.2.

Here, we present the MAP approach in a more general framework, and provide some practical suggestions on how to actually obtain the level curves on achievable regions.

The physics behind any MAP is, in principle, fairly simple: the driver controls the angular position δ_v of the steering wheel, and the forward speed u , and the vehicle reacts with a lateral velocity v and a yaw rate r . Mathematically, it means that the steady-state behavior of any vehicle is completely characterized by two maps¹

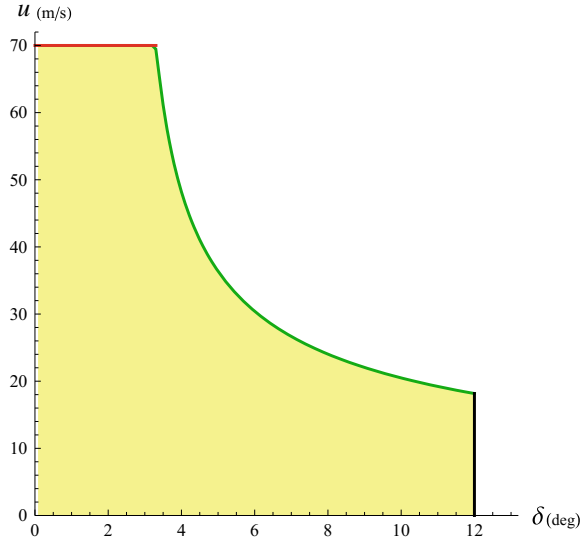
$$v = \hat{v}(\delta_v, u) \quad \text{and} \quad r = \hat{r}(\delta_v, u) \tag{6.43'}$$

The use of v and r to monitor the vehicle behavior is not mandatory. In fact, to have a more geometric description of the vehicle motion, we prefer to use $\beta=v/u$ and $\rho=r/u$

¹In this chapter some subscripts are dropped to make equations more readable.

The original version of this chapter was revised: Belated corrections have been incorporated. The correction to this chapter is available at https://doi.org/10.1007/978-3-319-73220-6_12

Fig. 8.1 Achievable region in the input space (δ, u) , with boundary $u_{lim}(\delta)$



$$\beta = \hat{\beta}(\delta_v, u) \quad \text{and} \quad \rho = \hat{\rho}(\delta_v, u) \tag{6.44'}$$

Of course, at steady-state all these quantities are constant in time.

Actually, a number of other interesting kinematic quantities can be mapped as well. They are all functions of (δ_v, u) . For instance, the lateral acceleration² $a_y = ur$ is certainly a must in vehicle dynamics.

8.2 Achievable Regions

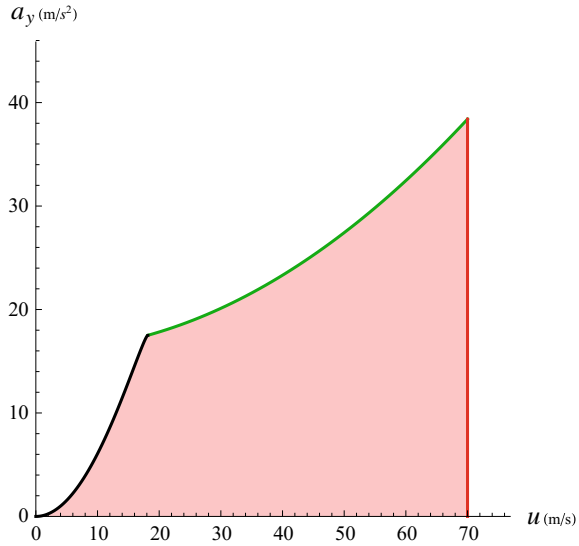
Several types of achievable regions can be associated to a given vehicle. They are in principle equivalent, in the sense that all of them refer to the same steady-state conditions. However, different regions help understanding different vehicle features.

8.2.1 Input Achievable Region

Let us start with the achievable region in the plane (δ, u) (Fig. 8.1), where $\delta = \tau\delta_v$, as in (3.66).

²In this chapter we use a_y for \tilde{a}_y .

Fig. 8.2 Achievable region in the space (u, a_y) , with boundary $a_{y,\text{lim}}(u)$



First, we observe that input quantities are subject to obvious practical limitations: maximum steer angle δ_{max} , and vehicle maximum speed u_{max} (12° and 70 m/s, respectively, in Fig. 8.1).

However, things are not so simple. The achievable region cannot be a rectangle. Owing to finite grip, the achievable forward speed is limited and depend on δ , as marked by the curved boundary $u_{\text{lim}}(\delta)$, connecting the two straight sides in Fig. 8.1.

As already stated, it is reasonable to assume that the driver controls the steering wheel angle δ_v and the forward speed u . However, in some cases it is useful to consider also the lateral acceleration a_y as a possible input quantity.

This aspect is more evident in the achievable region in the plane (u, a_y) , shown in Fig. 8.2. We see that at low speeds the lateral acceleration a_y is limited by the maximum steer angle, while at medium to high speeds, a_y is grip limited. The achievable region in Fig. 8.2 has a speed dependent boundary $a_{y,\text{lim}}(u)$, clearly showing that we are dealing with a Formula car with relevant aerodynamic downforces.

Also interesting is the achievable region in the plane (δ, a_y) , shown in Fig. 8.3 for the same Formula car. At small steer angles, the boundary is due to u_{max} , while for medium to high values of δ , the lateral acceleration is limited by the grip and by the aerodynamic downforces.

All these figures, unless otherwise specified, are for a simple mathematical model of an understeer vehicle with wings and open differential (basically a Formula car at the center of a bend).

More formally, we have from Fig. 8.3 that

$$\delta_{\text{lim}}(u) = \delta(a_{y,\text{lim}}(u), u) \tag{8.1}$$

which can be inverted to get (Fig. 8.1)

$$u_{\text{lim}}(\delta) \tag{8.2}$$

Fig. 8.3 Achievable region in the space (δ, a_y) , with boundary $a_{y,\text{lim}}(\delta)$

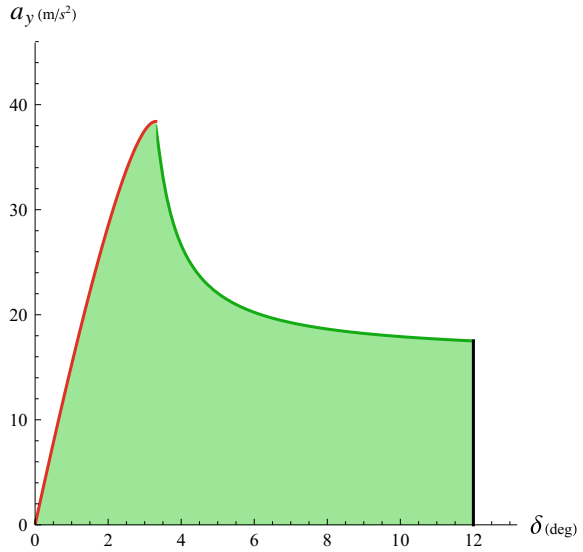
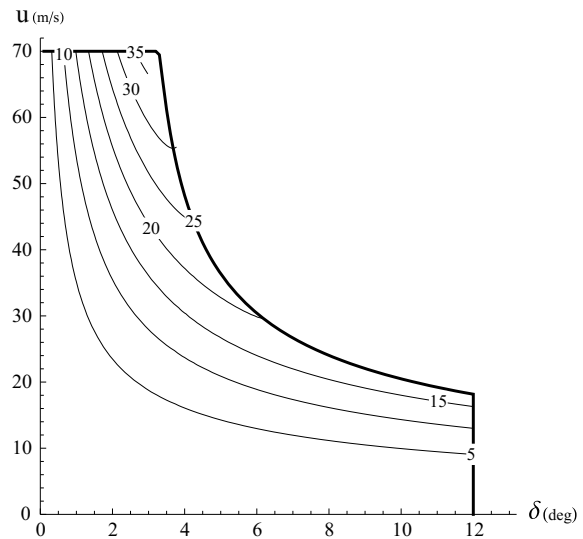


Fig. 8.4 Achievable input region (δ, u) , with level curves of constant lateral acceleration a_y (m/s^2)



and hence, as shown in Fig. 8.3

$$a_{y,\text{lim}}(\delta) = a_{y,\text{lim}}(u_{\text{lim}}(\delta)) \tag{8.3}$$

These functions define the boundary of input achievable regions. Moreover, they are also useful for obtaining the boundaries of output achievable regions.

Fig. 8.5 Achievable input region (u, a_y) , with level curves of constant steer angle δ (deg)

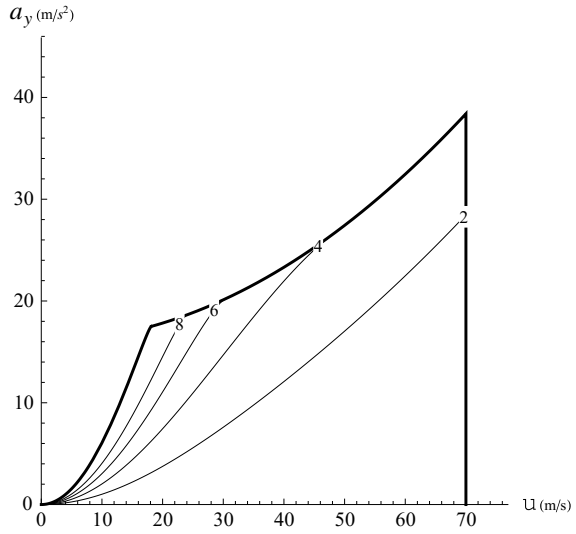
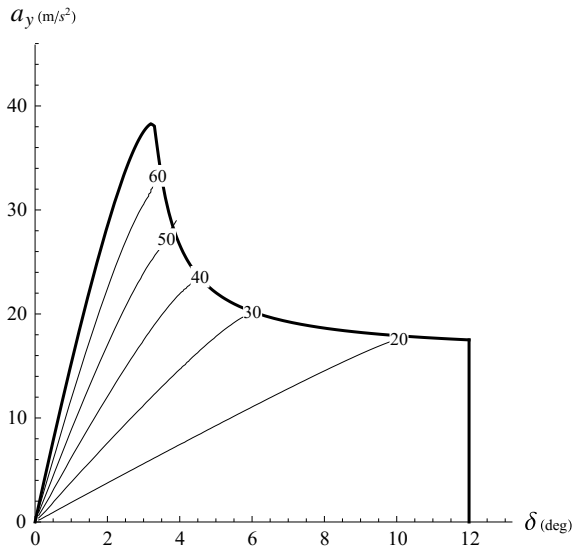


Fig. 8.6 Achievable input region (δ, a_y) , with level curves of constant forward speed u (m/s)



It is very important to realize that all these input regions cover exactly the same set of steady-state working conditions of the vehicle. However, to really make these region fully equivalent it is necessary to draw the level curves for the corresponding “missing” quantity, as done in Figs. 8.4, 8.5 and 8.6. We invite the reader to check that these three MAPs are indeed equivalent.

Aerodynamic devices affect pretty much the shape of achievable regions, as shown in Fig. 8.7. Each region highlights different effects on the vehicle behavior.

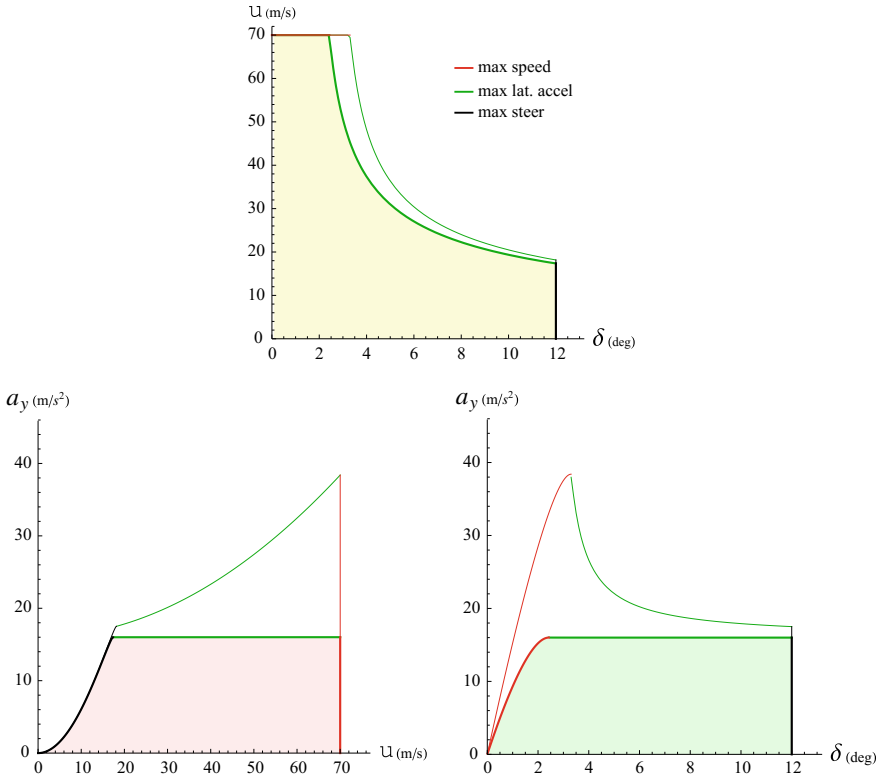


Fig. 8.7 Comparison of achievable regions with and without aerodynamic downloads

Also interesting is comparing vehicles with different level of understeer, as done in Fig. 8.8. Again, the three regions change in different ways. Of course, it takes time to get used to this approach to analyze the handling behavior.

8.2.2 Output Achievable Regions

Output achievable regions are, by definition, the image of input achievable regions.

For instance, in the plane (ρ, β) we have a region like in Fig. 8.9. As expected, the boundary is made up of four parts (see also Fig. 6.30): maximum steer angle, limit lateral acceleration, maximum speed, and (almost) zero speed.

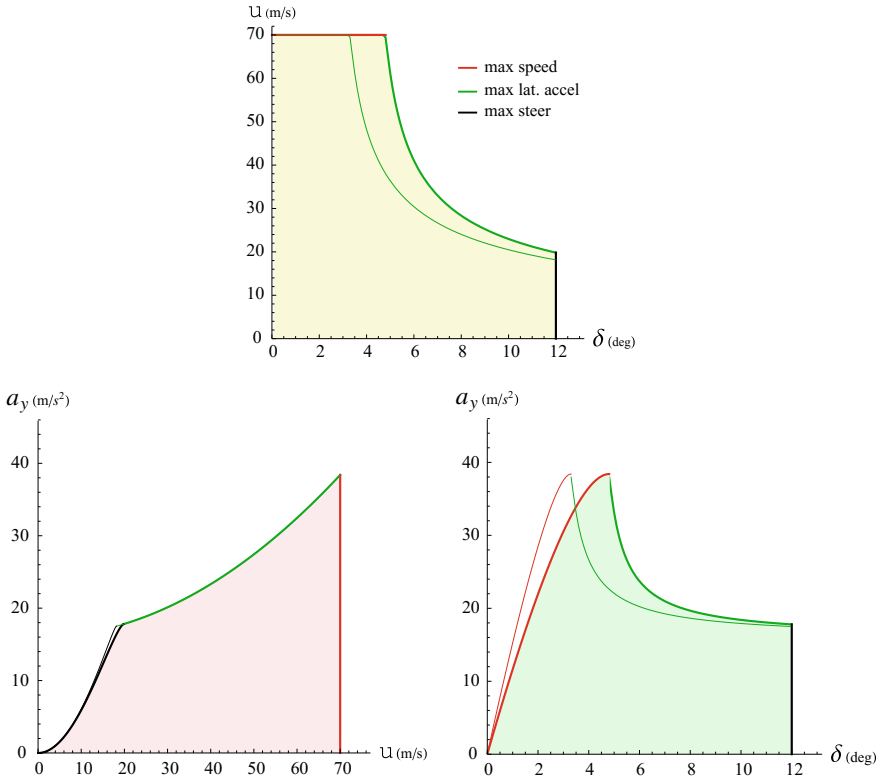


Fig. 8.8 Thick lines are for a more understeer race car

Fig. 8.9 Output achievable region in the plane (ρ, β)

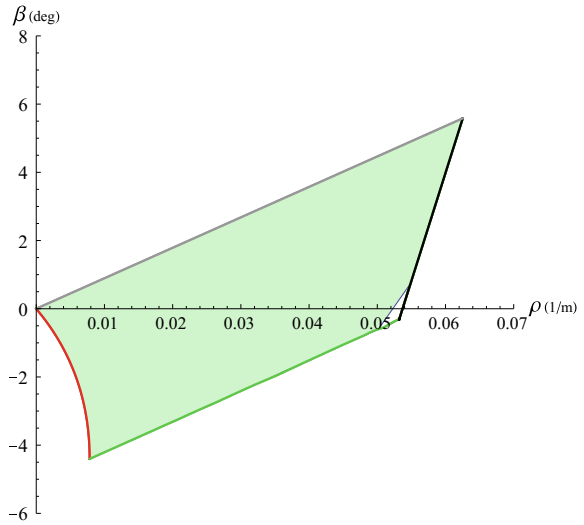
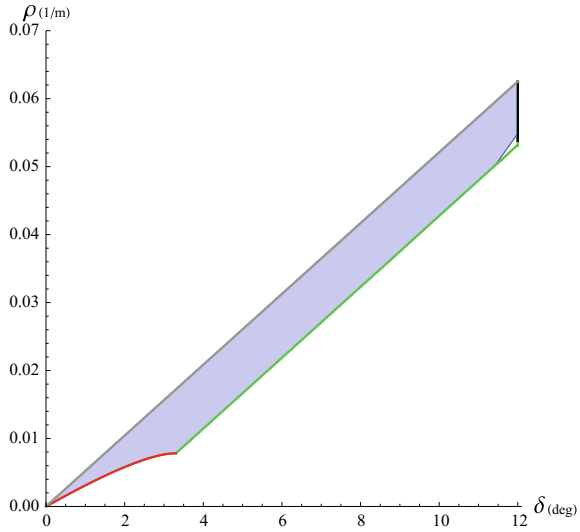


Fig. 8.10 Mixed I/O achievable region in the plane (δ, ρ)



8.2.3 Mixed I/O Achievable Regions

Also mixed input/output achievable regions are possible. For instance, in the plane (δ, ρ) we have a region like in Fig. 8.10. Again, the boundary is made up of four parts: maximum steer angle, limit lateral acceleration, maximum speed, and (almost) zero speed (see also Fig. 6.42).

8.3 Achievable Performances on Input Regions

Level curves of any measurable or computable quantity can be drawn inside an input achievable region. For instance, lines at constant β and constant ρ are shown in Fig. 8.11. The same kind of lines are drawn in Fig. 8.12 and also in Fig. 8.13. These plots look at first very different, but provide, if combined with Figs. 8.5 and 8.6, the same information on the steady-state behavior of the vehicle.

Incidentally, we observe that $\beta \simeq -4^\circ$ characterizes part of the boundary.

We remark that *level curves* of any physical quantity can be drawn on input achievable regions. For instance, in Figs. 8.14 and 8.15, we see level curves for constant damping ratio ζ , defined in (6.131), and constant damped natural frequency ω_s (rad/s), defined in (6.131). We have at a glance a clear and complete picture of how the dynamic features of the vehicle evolve when changing the steer angle δ , the forward speed u and the lateral acceleration a_y . In the lower part of the achievable regions the vehicle behavior is overdamped and hence not oscillatory. On the other hand, when approaching the a_y limited boundary the damping ratio tends to zero.

To better appreciate the interplay between ω_s and ζ , we can draw the achievable region in the plane (ω_s, ζ) (Fig. 8.16), with red lines at constant speed and black lines

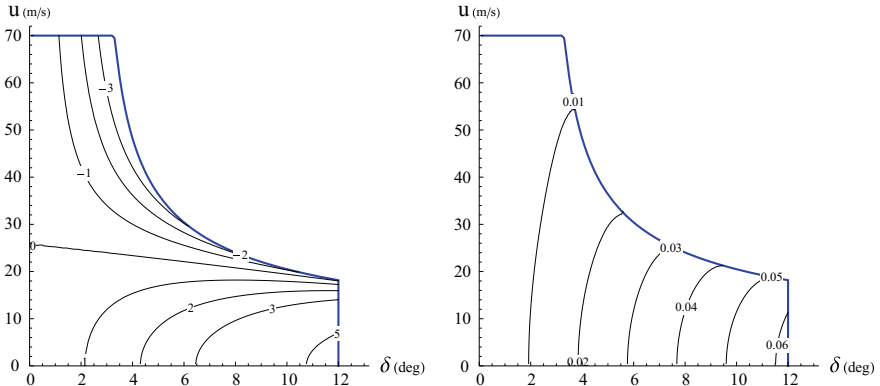


Fig. 8.11 Level curves for constant β (left) and ρ (right)

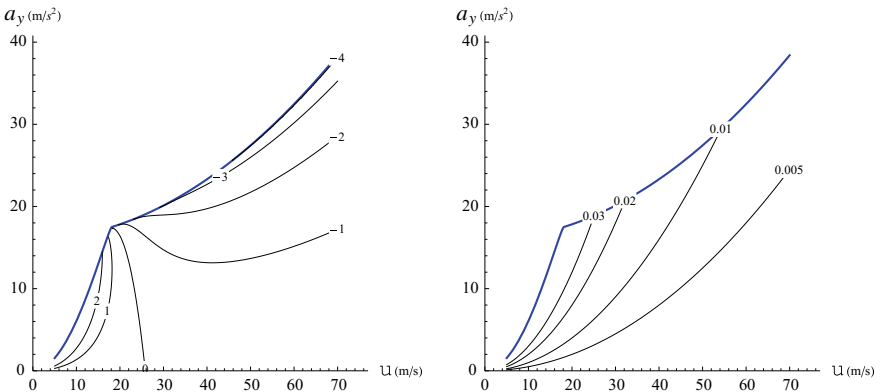


Fig. 8.12 Level curves for constant β (left) and ρ (right)

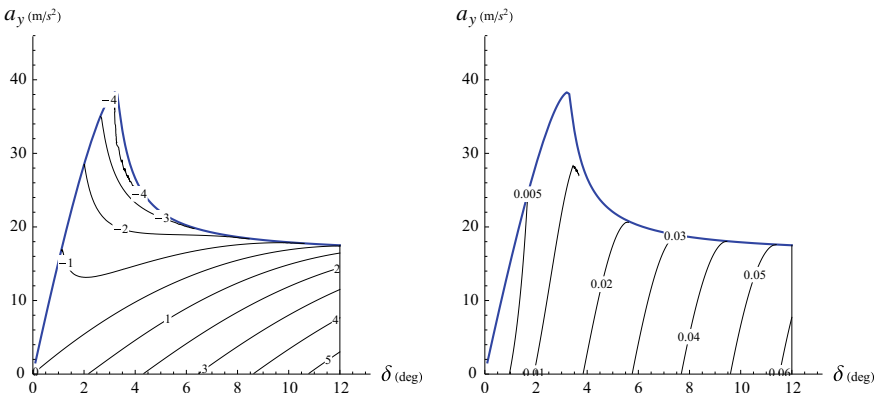


Fig. 8.13 Level curves for constant β (left) and ρ (right)

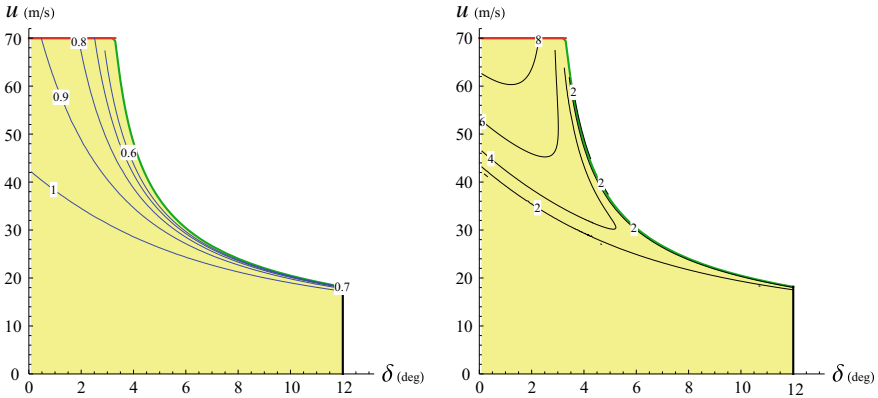


Fig. 8.14 Level curves for constant damping ratio ζ (left) and constant damped natural frequency ω_s (right)

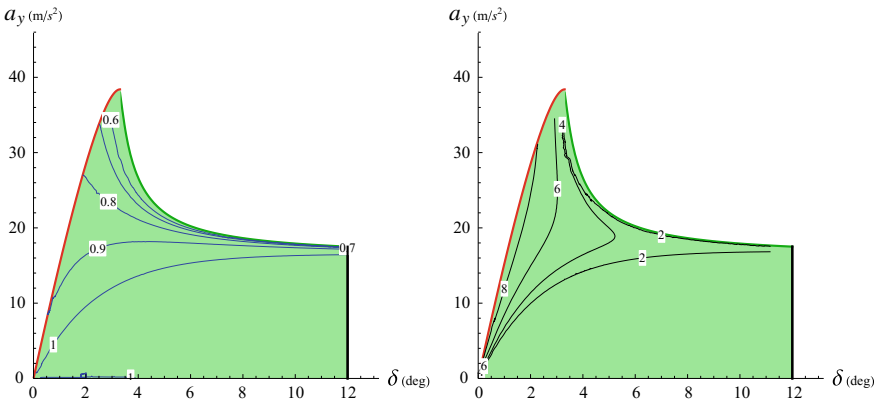


Fig. 8.15 Level curves for constant damping ratio ζ (left) and constant damped natural frequency ω_s (right)

at constant steer angle. Of course, this achievable region only covers the oscillatory behavior of the vehicle.

Other noteworthy examples may be stability derivatives, control derivatives, gradients, lateral forces, etc. Therefore, achievable *input* regions appear to be a very general way to monitor vehicle performances.

8.4 Achievable Performances on Output Regions

On the output region (ρ, β) it is useful and fairly easy to draw parametric curves keeping constant one input parameter (Fig. 8.17). Therefore, we have curve with constant forward speed u , constant steer angle δ_v , and constant lateral acceleration a_y .

Fig. 8.16 Level curves for constant δ (black lines) and constant u (red lines) in the plane (ω_S, ζ)

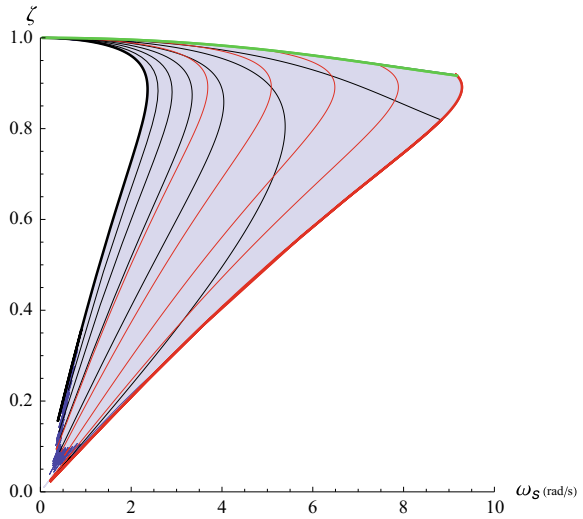
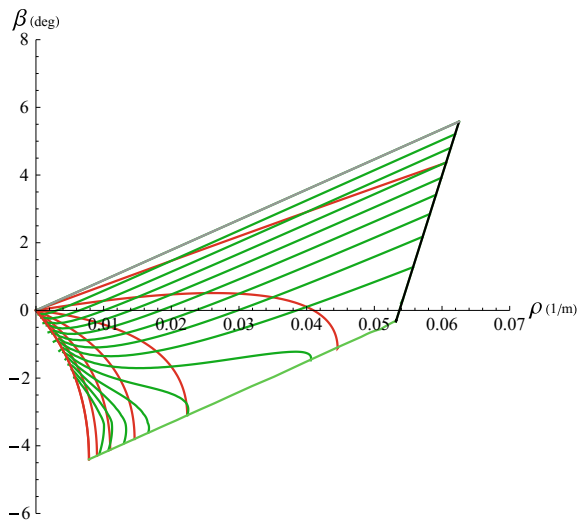


Fig. 8.17 Level curves for constant u (red lines) and constant a_y (green lines) in the output plane (ρ, β)



It is much more difficult to keep constant some other output quantity. The same observations hold true also for mixed I/O regions.

8.5 Achievable Performances on Mixed I/O Regions

The plane (δ, ρ) is perhaps the most intuitive MAP (Fig. 8.18), particularly if we draw level curves for constant speed u . It immediately shows how a driver can operate on δ and on u to negotiate a bend with curvature ρ .

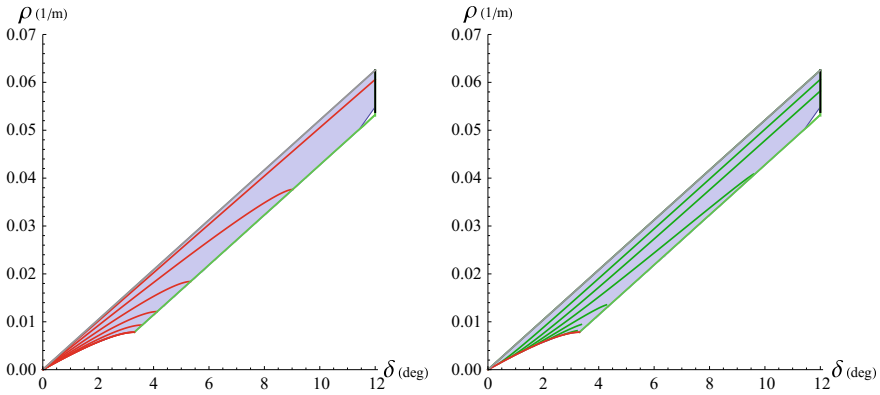


Fig. 8.18 Level curves for constant speed u (left) and constant lateral acceleration a_y (right) in the plane (δ, ρ)

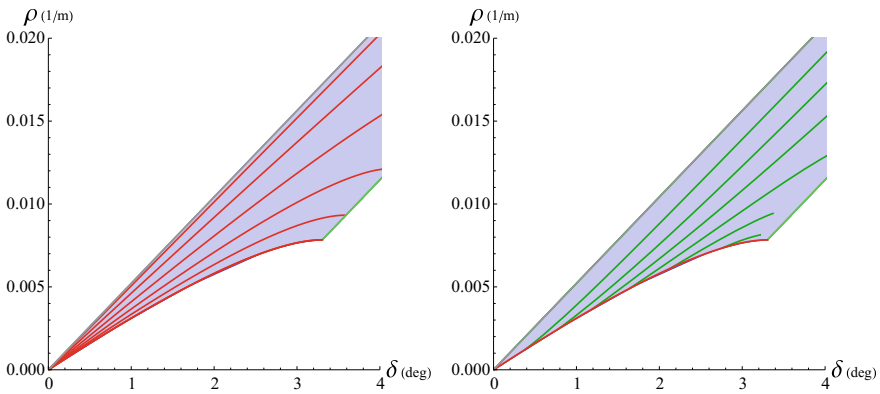


Fig. 8.19 Closeup of level curves for constant speed u (left) and constant lateral acceleration a_y (right) in the plane (δ, ρ)

Also interesting is the closeup of Fig. 8.19 for high speeds, which clearly shows the interplay between u and a_y in a car with aerodynamic devices.

8.6 MAP from Slowly Increasing Steer Tests

All the MAPs presented so far in this Chapter were obtained with a single track model with aerodynamic downloads. Now, it is time to employ a more realistic double track model, still for a Formula car, as it were a real vehicle to be tested on a proving ground.

The so-called Slowly Increasing Steer (SIS) test is a good way to collect (pseudo) steady-state data. To span several working conditions, we perform the test at several

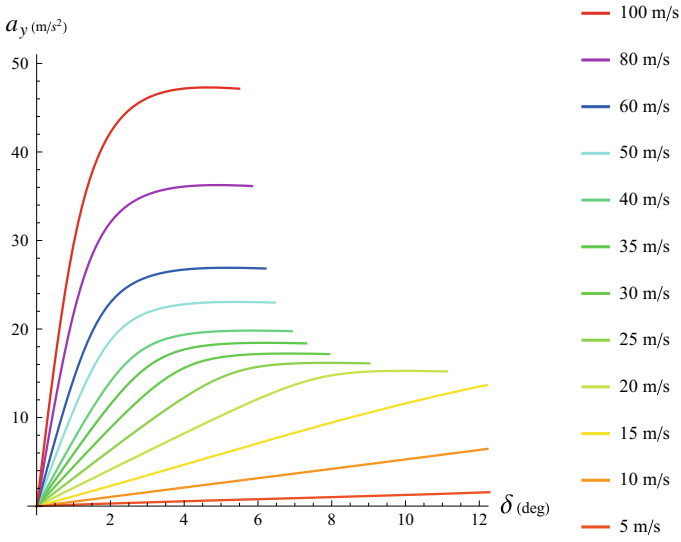


Fig. 8.20 MAP (δ, a_y) with level curves for constant u

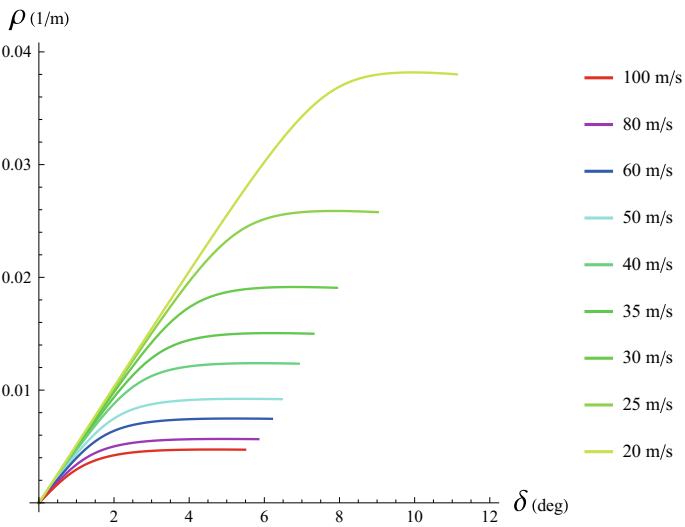


Fig. 8.21 MAP (δ, ρ) with level curves for constant u

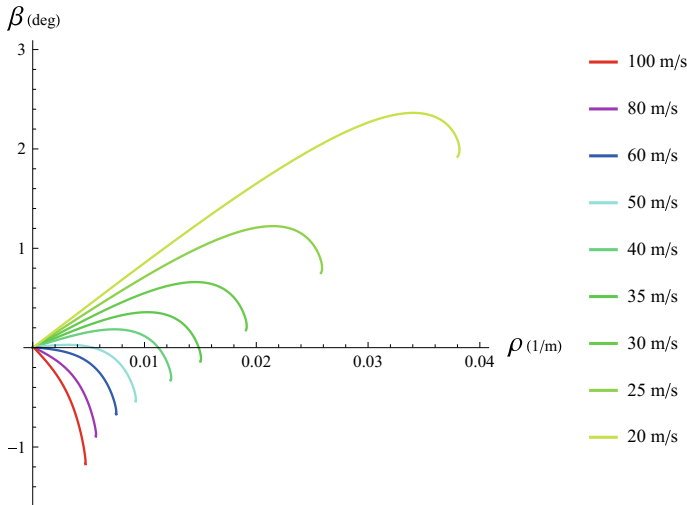


Fig. 8.22 MAP (ρ, β) with level curves for constant u

different constant forward speeds u . In all cases, we increase the front wheel steer angle δ , starting from zero, with a constant rate of 0.5 deg/s.

Three possible MAPs with level curves for constant forward speed u are shown in Figs. 8.20, 8.21 and 8.22. We can easily infer the shape of the corresponding achievable regions.

8.7 MAP from Constant Steer Tests

Useful MAPs can also be obtained from tests with constant steer angle and slowly increasing speed. Actually, this is the most robust test procedure: keeping constant the steering wheel position is easy, and certainly easier than keeping constant the forward speed, not to mention how hard it is to keep constant the turning radius.

Again, in Fig. 8.23 the shape of the achievable region is clearly defined. Moreover, we observe that at sufficiently high speed, the boundary of the achievable region can be reached with values of δ as low as about 4 degrees.

Also interesting is adding the constant steer lines to Fig. 8.22, thus obtaining Fig. 8.24. Maybe, this is the MAP that better highlights the different handling features of this race car when “visiting” different points inside the achievable region.

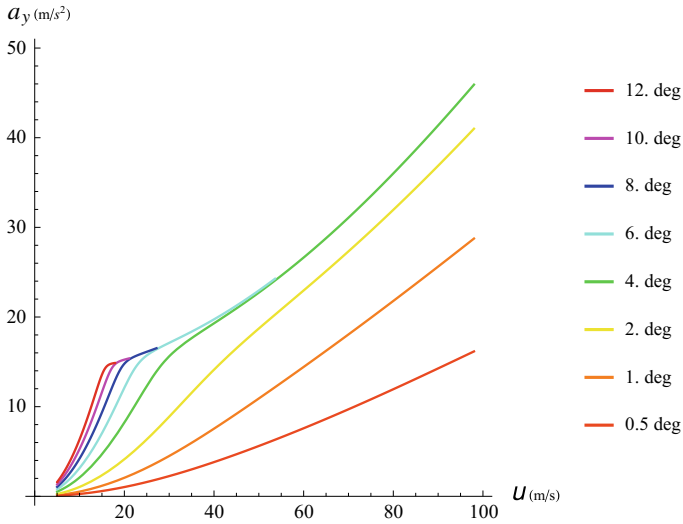


Fig. 8.23 MAP (u, a_y) with level curves for constant δ

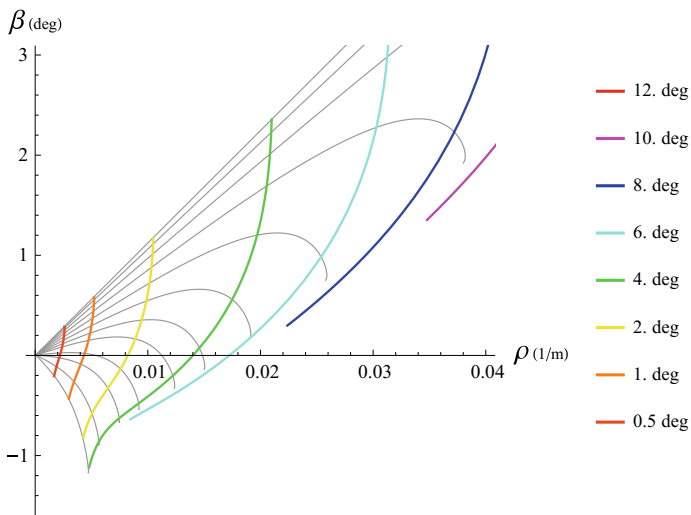


Fig. 8.24 MAP (ρ, β) with also level curves for constant δ

8.8 Concluding Remarks

The MAP approach looks promising, but it still needs to be fully developed to become a way to really compare different setups. We have to understand how to read these plots. We have to learn what to look at and why. This is to say that we should refrain from discarding the MAP approach just because it has not provided very good answers in a while.

8.9 Key Symbols

a_y	lateral acceleration
r	yaw rate
u	longitudinal velocity
v	lateral velocity
β	v/u
δ	$\tau\delta_v$ (net steer angle of the wheels)
δ_v	angular position of the steering wheel
ζ	damping ratio
ρ	r/u
τ	gear ratio of the steering system
ω_s	damped natural frequency